Triggering and Relationship Between Mine Earthquake Activities and Stress of Earth Tides During Deep Mining

Yuezheng Zhang[1,2]*, Hongguang Ji[1,2] and Haoyuan Wu[1,2]

[1]University of Science and Technology Beijing, Beijing, China, [2]Beijing Key Laboratory of Urban Underground Space Engineering, Beijing, China

In the process of deep mining, the prevention and control of rock bursts, mine earthquakes, and other disasters are common problems. The stress of earth tides and its periodic actions should trigger mine earthquakes when the rock masses are in a critical state of rupture. In this study, the Yanbei coal mine was taken as the research background to explore the triggering effect of solid tides on mine earthquakes occurring in the floor. The relationship between the diurnal tidal stress phase and mine earthquakes was studied by statistically analyzing the mine earthquake frequency, and the triggering mechanism was also preliminarily discussed. It was found that the solid tide plays a significant role of trigger action in the occurrence of rock burst of the floor type. For different levels of mine earthquakes, the tidal stress triggering effect is different, but the overall trend is close. Compared with the components of tidal stress, vertical stress, north-south stress, and shear stress, rock burst occurred more at the stage close to $0°$ and $\pm180°$. For different types of mine earthquakes, the triggered mechanics function of tidal stress is different. Mine earthquakes on the floor mainly include two kinds (the gravity control type and horizontal stress control type). The former easily occurs during the tidal stress vertical component of the maximum, while the latter easily occurs when the two horizontal components of the maximum are combined. The frequency of the former is larger than that of the latter. The results show that the floor seismic activity is correlated with the solid tidal activity of the earth's crust, which provides a new idea for understanding the mechanism and trigger conditions of mine earthquakes.

Keywords: coal mine, mine earthquake, tidal stress, floor, trigger mechanism

INTRODUCTION

Mine earthquakes occur under the combined effects of the geological structure environment, the geostress field, and other occurrence environments and mining disturbances. When the engineering rock mass reaches a critical state, a small disturbance will have an important impact on it, thereby promoting the occurrence of rock mass destruction (Feng et al., 2015; Xie et al., 2015; Zhang et al., 2016a). For example, in the local earth tidal activity, the action of tidal forces will form an additional stress field in the geostress field (Pan et al., 2020; Yuan, 2021). Luo et al. (2015) studied the effect of tidal force on coal and gas outbursts and found that there is a certain correlation between coal and gas outbursts and the tidal force of celestial bodies. The tidal force has a certain driving effect on the occurrence of outbursts. Li et al. (2011) also found that the occurrence of mine earthquakes was concentrated in local time periods when the statistics of the frequency distribution of mine earthquakes occurred. When analyzing the time of occurrence of rock bursts and the correlation between regions and changes in tidal force, Guo and Yang, (2021) found that the probability
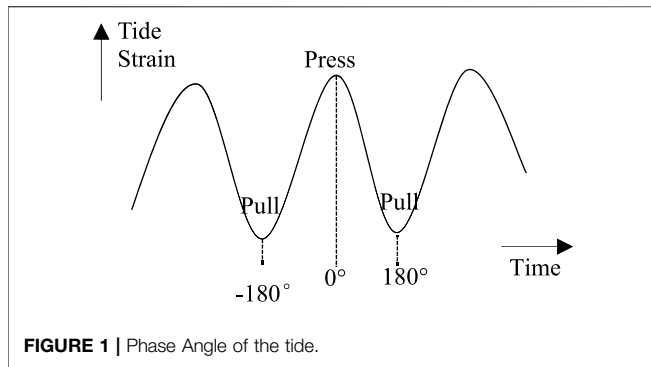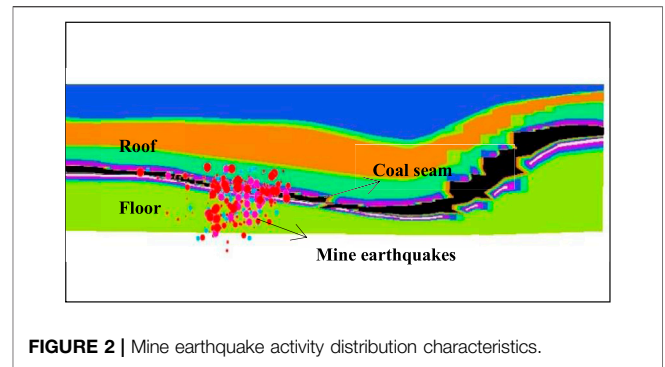
FIGURE 1 | Phase Angle of the tide.

FIGURE 2 | Mine earthquake activity distribution characteristics.

and frequency of rock bursts occur more frequently in the period of extreme tidal generating force. It is found that there is a certain relationship between the area where mine earthquakes occur and the latitude and longitude. Seismic research has also confirmed that it has a certain triggering effect on earthquakes, which is mainly reflected in that when the tectonic stress in the source system rock reaches or is in a critical state; external factors such as earth tide modulation may cause system mutation and earthquakes under certain conditions (Glasby and Kasahara, 2001; Chen et al., 2006; Metivier et al., 2009; Li et al., 2014; Wu et al., 2020). According to Zhang et al. (2016b) statistics on roof-type mine earthquakes, it is found that solid tidal stress has a significant triggering effect on the occurrence of mine earthquakes. In recent years, with the development and application of technologies (such as roof control, roadway surrounding rock support, and pressure relief), floor impact dynamic disasters have become more prevalent. The impact damage to the floor directly causes serious damage and threat to the equipment and personnel lanes, and the impact on production safety is even more serious. As a critical phenomenon of multi-field evolution and coupling, floor-type mine earthquakes are induced during their transition from incubation to induction. The effect and mechanism of tidal stress on floor-type mine earthquakes need to be further explored.

In order to quantitatively analyze the correlation between earth tide action and induced floor-type mine earthquakes, the correlation of vertical, east-west, north-south, and north-south diurnal variation was studied by monitoring the earthquake in Yanbei coal mine in Gansu province. The magnitude and type of horizontal shear stress, local solid tidal stress, and floor type mine earthquake are analyzed. The inducing effect and mechanical mechanism of the earth's tide factors on the floor-type mine earthquakes are preliminarily discussed.

CHARACTERISTICS OF REGIONAL TECTONIC STRESS AND SOLID TIDAL STRESS

The Yanbei mining area in Gansu province is located at the eastern foot of the Liupan mountain and the southwestern edge of the Ordos block. It is at the intersection of the Liupanshan western marginal fault, the western marginal thrust belt of the Ordos Basin, and the Qingtongxia-Guyuan fault. The geological environment in this area is complex, and the tectonic stress is concentrated. The coalfield area has been subjected to structural compression from southwest to northeast and east to west for a long time, forming a spinning compound asymmetric synclinal structure of the "southeast structure, slow in the east and steep in the west, wide and slow in the middle, and converging in the north and south sections".

Under the action of the tide, the tidal force generated by the tidal force at different times and locations is different. The stress field in the formation will change periodically with a certain regularity, that is, the tidal additional stress field. The tidal force level calculation is shown in **Eqs 1–3** (Zahran et al., 2005; Kano and Yanagidani, 2006; Chen et al., 2012):
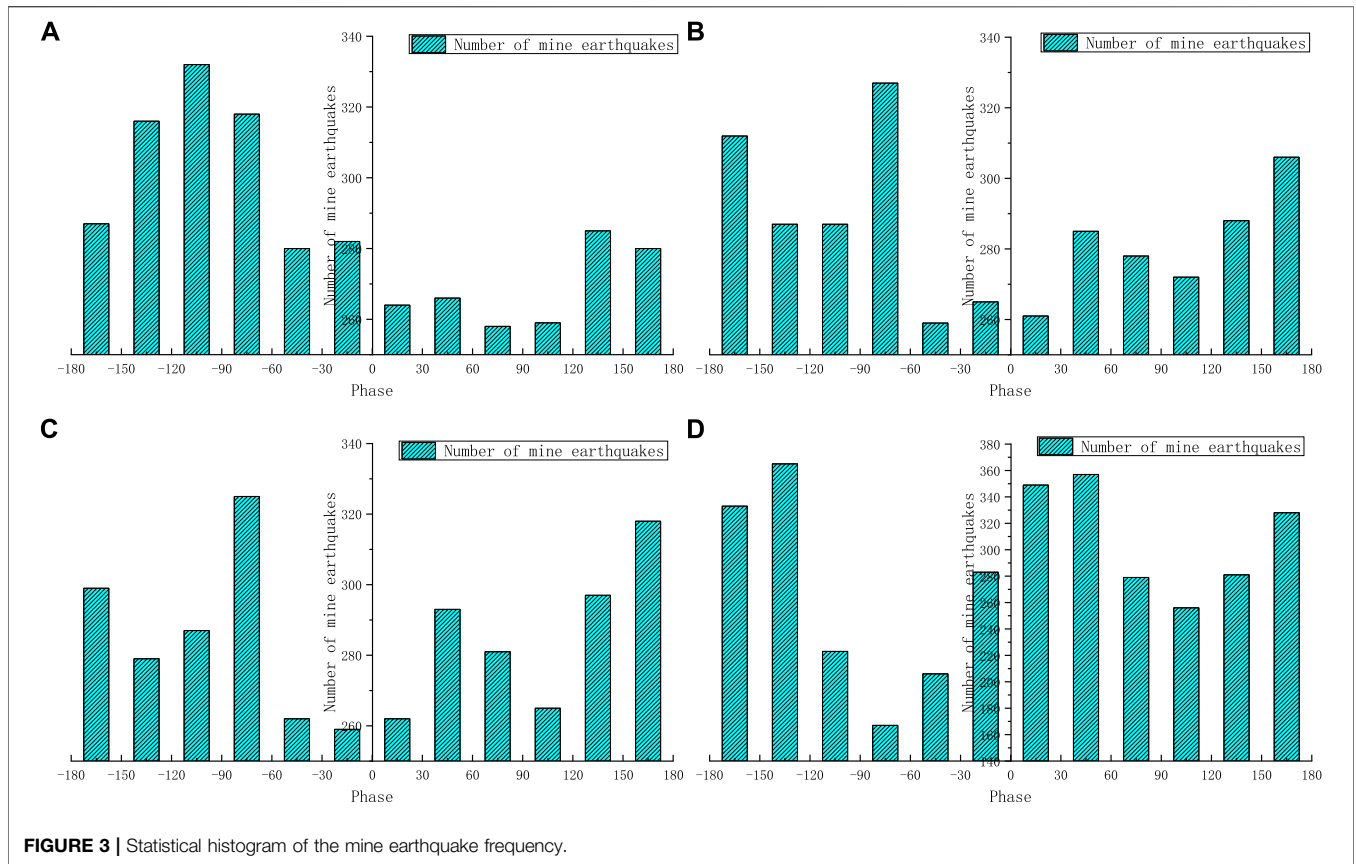
$$W = W_m + W_s, \tag{1}$$

$$W_m = D_m\left(\frac{r}{R}\right)^2\left[2\left(\frac{c_m}{r_m}\right)^3\left(\cos^3 z_m - \frac{1}{3}\right) + \frac{2}{3}\frac{r}{c_m}\left(\frac{c_m}{r_m}\right)^4\left(5\cos^3 z_m - 3\cos z_m\right)\right], \tag{2}$$

$$W_s = D_s\left(\frac{r}{R}\right)^2\left[2\left(\frac{c_s}{r_s}\right)^3\left(\cos^3 z_m - \frac{1}{3}\right)\right]. \tag{3}$$

W is the tidal force position; W_m and W_s are the moon and solar tidal force; D_m and D_s are Moon and Sun Dudson's constant; c_m and c_s are the average distance from the moon; r_m and r_s are the distance from the Sun to the center of the earth; z_m and z_s are the distance from the moon and that from the Sun to the center of the earth; R is the average radius of the earth.

The variable component of the solid tide is also related to the Love-Shida's number, and its calculation formula is as follows:

$$\begin{cases} e_{rr} = \sum_n \left(R\frac{\partial h_n}{\partial r} + nh_n\right)\frac{w_n}{Rg_0}, \\ e_{\phi\phi} = \sum_n \left(\frac{l_n}{Rg_0}\frac{\partial^2 W_n}{\partial\phi^2} + h_n\frac{w_n}{Rg_0}\right), \\ e_{\lambda\lambda} = \sum_n \left[\frac{l_n}{Rg_0\cos\phi}\left(\frac{\partial^2 W_n}{\cos\phi\partial\lambda^2} - \sin\phi\frac{\partial W_n}{\partial\phi}\right) + h_n\frac{w_n}{Rg_0}\right], \\ e_{\phi\lambda} = \sum_n \left[\frac{-2l_n}{Rg_0\cos\phi}\left(\frac{\partial^2 W_n}{\partial\phi\partial\lambda} + \tan\phi\frac{\partial W_n}{\partial\lambda}\right)\right]. \end{cases} \tag{4}$$

FIGURE 3 | Statistical histogram of the mine earthquake frequency.

e_{rr}, $e_{\phi\phi}$, $e_{\lambda\lambda}$, and $e_{\phi\lambda}$ are the vertical, north-south, east-west, and horizontal shear stress components of the solid tidal strain; l_n and h_n are the Love-Shida's number; ϕ latitude; λ longitude.

According to the relationship between stress and strain, the components of the corresponding solid tidal stress can be further obtained (Zhou et al., 2013; Xiong et al., 2015):

$$\sigma_{ij} = \lambda'\vartheta\delta_{ij} + 2\mu e_{ij}. \tag{5}$$

λ', μ, is the Lame constant at r, ϑ is the strained volume expansion, and δ_{ij} is the Kronecker symbol.

SCHUSTER TEST METHOD

Through calculation, the local tidal stress time history curve can be obtained. The triggering effect of the earth tide on the mine earthquake can be quantitatively analyzed by the change of P in the Schuster test method (Sun et al., 2014; Bucholc and Steacy, 2016; Zhu et al., 2021). P rejects the significance level of the null hypothesis (mine earthquakes occur randomly and have nothing to do with the tidal phase angle); the value range is 0–1. The smaller the value, the greater is the possibility of rejecting the null hypothesis. Taking $p < 0.05$ as the threshold for judging that the tide can trigger an earthquake, the calculation process is as follows.

The phase angle at the time of the earthquake is assigned according to the time-history of tidal stress, and the stress peak closest to the time of the earthquake is selected. The phase angle is 0°, and the phase angles in front of the tank and behind the tank are −180° and 180° respectively. Then, the angular distance is divided between the peaks and valleys linearly, as shown in **Figure 1**.

After determining the tidal phase angles of all earthquakes, the dominant phase angles of all seismic data are calculated, as shown in **Eq. 6**:

$$L = \sqrt{A^2 + B^2}, \tag{6}$$

$$A = \sum_{i=1}^{N}\cos\theta_i, \ \ B = \sum_{i=1}^{N}\sin\theta_i, \tag{7}$$

where θ_i represents the tidal phase angle of the first earthquake, N is the total number of earthquakes, and the value of P is calculated according to **Eq. 8**:

$$P = \exp\left(-\frac{L^2}{N}\right). \tag{8}$$

CORRELATION ANALYSIS BETWEEN THE SOLID TIDAL ACTION AND MINE EARTHQUAKE ACTIVITY

Figure 2 shows the source location results of some mine earthquakes (which induced rock burst events) in the

FIGURE 4 | Statistical histogram of the mine earthquake $M_L < 0$ frequency.
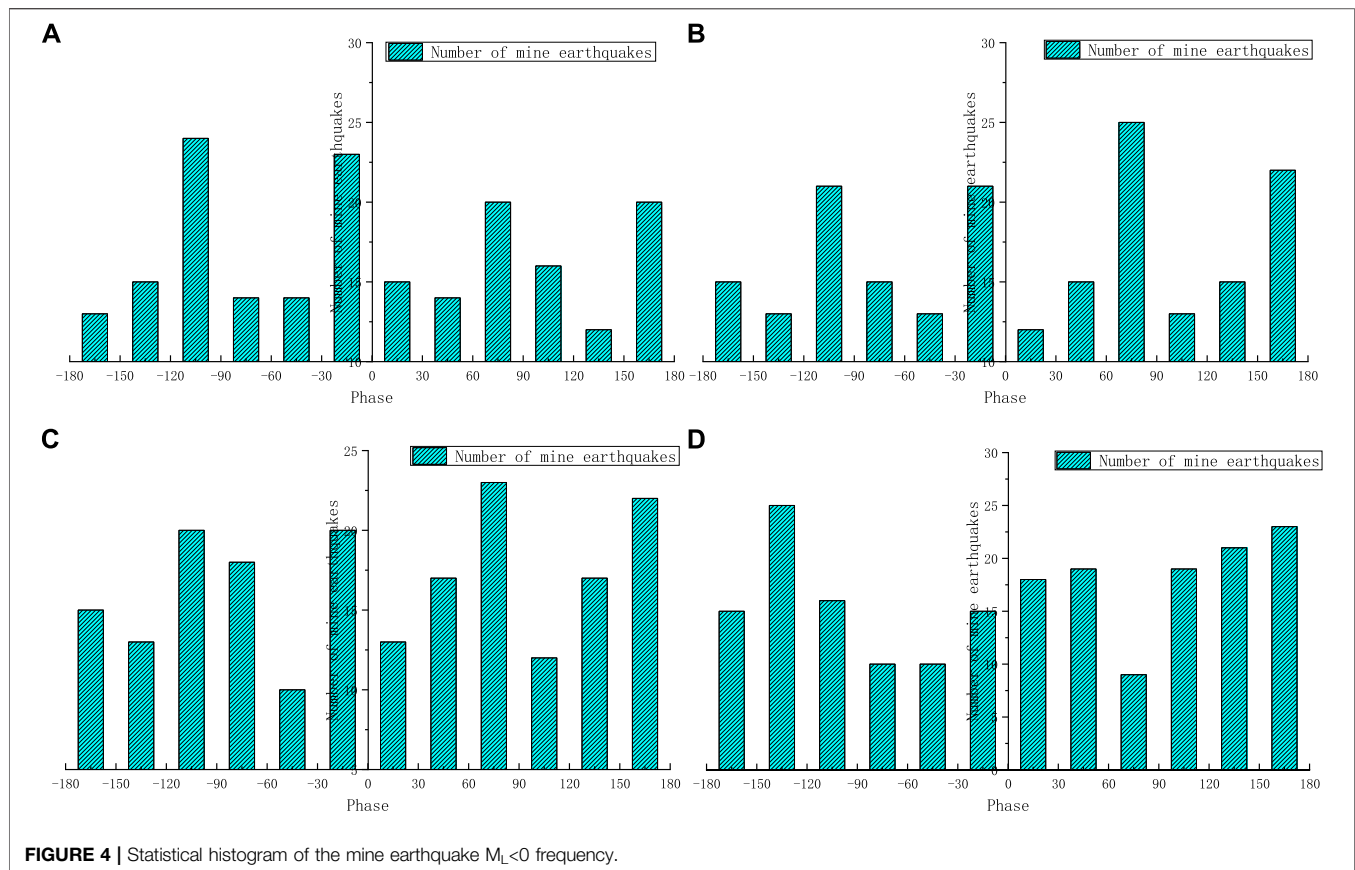
stratigraphic section perpendicular to the syncline axis. It can be seen that mine earthquakes are distributed in the rock layers above and below the coal seam. Different types of mine earthquakes have different formation mechanisms, and their triggering factors are also different. Compared with the mining face location, mine earthquakes can be divided into the roof type and floor type (Li et al., 2006). According to the damage records caused by rock bursts, mine shocks that occur in the floor often cause more serious damage. Therefore, in order to analyze the correlation between mine earthquakes and tidal stress, more than 30,000 floor-type mine earthquakes that occurred in this area are mainly selected as the analysis objects.

## Triggering Effect of Different Components of Tidal Stress on Mine Earthquakes

The study is based on the local strain solid tidal stress of the Yanbei coal mine, while selecting the vertical component, east-west component, north-south component, and horizontal shear stress component of the solid tidal stress as the tidal curve, respectively, to calculate the phase angle between the mine earthquakes in the Yanbei coal field and the tidal component. According to the interval of 30°, statistics of the mine earthquake data between −180° and +180° are carried out on a histogram. The statistical results are shown in **Figure 3**. Among them, (a), (b), (c), and (d) are the statistical results relative to the vertical, east–west,

north–south, and horizontal shear stress components, respectively.

It can be seen from **Figure 3** that in different components of tidal stress, there is a clear correlation between the frequency and phase angle of mine earthquakes in the floor. Compared with the vertical component, mine earthquake events are more distributed in the phase range near −100°, followed by the frequency near +150° phase and less frequently near 0°–90° phase. Compared with the north-south and east-west horizontal components, mine earthquake events are more distributed near the −75°phase; fewer events occur near the ±180° phase, and the least occur near the 0°phase. Compared with the horizontal shear component, there are more events near the 0° phase and ±180° phase and fewer events near the −70° phase. At the same time, compared to the Schuster test for the four tidal curves, the p values obtained are 1.32E−04, 0.0281, 0.0595, and 2.91E−07, respectively, and since the p values of each component are all lower than the threshold value of 0.05 for tidal-triggered earthquakes but north–south, it can be considered that the floor-type mine earthquakes in this area are triggered by tides.

Analysis of the Triggering Effect of Tidal Stress on Mine Earthquakes of Different Magnitudes

In earthquake research, it is found that solid tides have more obvious inducing effects on small-scale earthquakes than natural

FIGURE 5 | Statistical histogram of the mine earthquake $0 \leq M_L < 0.5$ frequency.
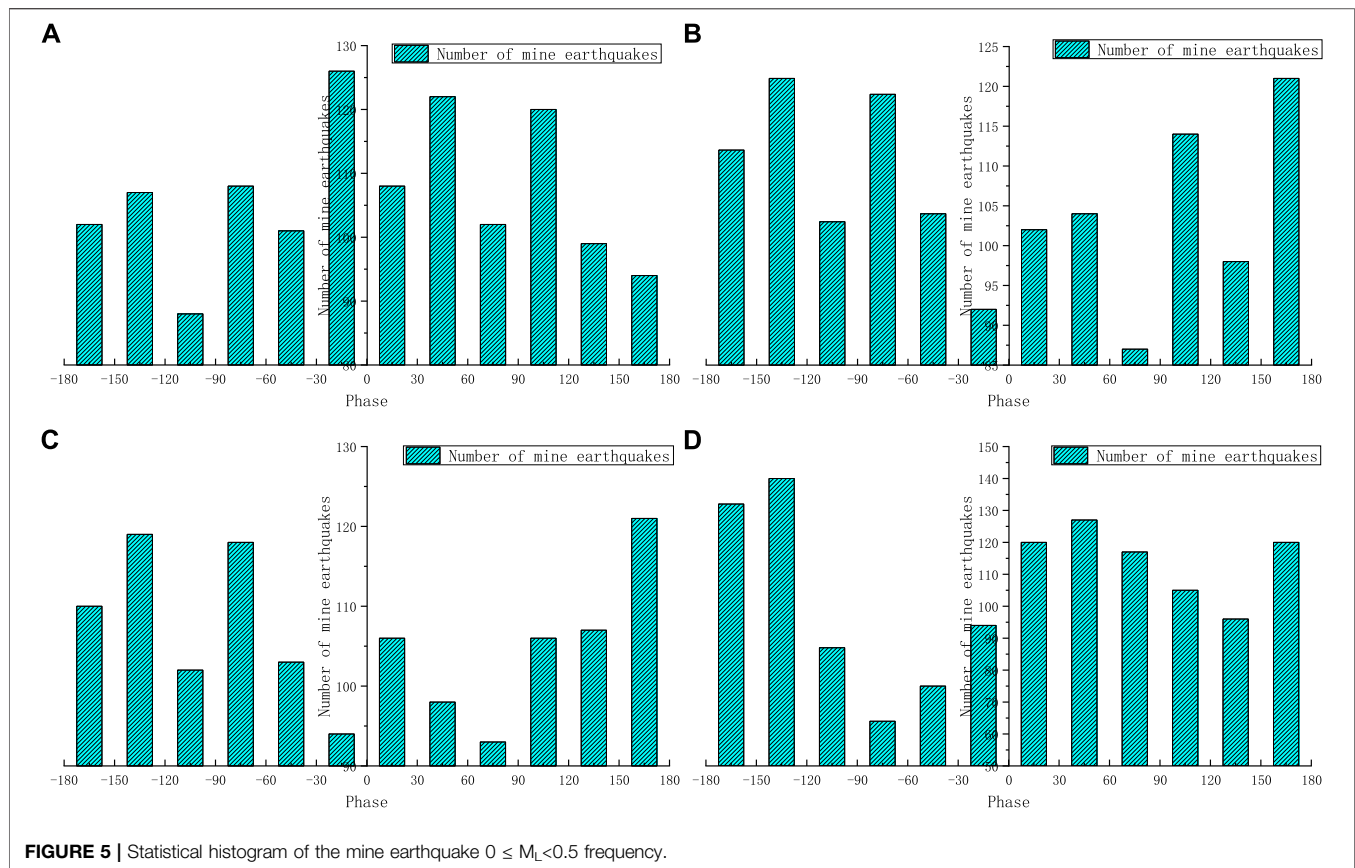
large earthquakes. For mine earthquakes, although the magnitude is low, the causes and triggering mechanisms of mine earthquakes of different scales are also different. In order to analyze the triggering effect and the difference in the earth's tide in the process of different scales of mine earthquakes, the mine earthquake events are divided into "<0, 0–0.5, 0.5–1.0, 1.0–1.5, and >1.5", according to the magnitude (M_L). **Figure 4** to **Figure 8**, respectively, show the corresponding relationship between the frequency of occurrence of different levels of mine earthquake events and the tidal phase. Among them, (a), (b), (c), (d) are the statistical results relative to the vertical, east-west, north-south, and horizontal shear stress components, respectively.

It can be seen from **Figure 4** that for the vertical component, mine earthquake events are more distributed in the phase range near 0° and ±90°, and few occur near the −180° phase. For the north–south and east–west horizontal components, mine earthquake events are more distributed near the 0° and ±90° phases, and few occur near the −60° and 100° phases. For the horizontal shear component, the events near the ±150° phase are the most, followed by the phase distribution near 30°, and the least events near the phases of −90°~ −30° and 60°–90°.

It can be seen from **Figure 5** that for the vertical component, mine earthquake events are more distributed in the phase range near 0°, and less occur near the ±180° phase. For the north–south and east–west horizontal components, mine earthquake events are more distributed near the ±180° phases, and less occur near the 0° phases. For the horizontal shear component, the law is

obvious. It is more distributed near 30°–60° and ±180°, and the events near −90°~−60° phase are the least.

It can be seen from **Figure 6** that for the vertical component, mine earthquake events are more distributed in the phase range around 0° and ±120°, and few occur near the phase of ±180°. For the north-south and east–west horizontal components, mine earthquake events are more distributed near the ±60° and ±180° phases, and few occur near the 0° phase. For the horizontal shear component, there are more events around the phases of 0° and ±180°, and the least phase events are around ±90°.

It can be seen from **Figure 7** that for the vertical component, mine earthquake events are more distributed in the phase range around −0° and +100°, but at near ±180°, +60° phases there is less occurrence. For the two horizontal components, north-south and east-west, there are more ore earthquake events near the phases of ±90°. For the horizontal shear component, there are more events around the phases of 0°–60°, and ±180°.

It can be seen from **Figure 8** that for the vertical component, mine earthquake events are more distributed in the phase range near the ±90° phase, and few occur near the ±60° phase. For the north–south and east–west horizontal components, mine earthquake events are more distributed near the ±90° phase, followed by near ±180°, and few occur near the ±120° phase. For the horizontal shear component, there are more events around the 0° phase, followed by the phase around +180°, and the least phase events around ±90°.

FIGURE 6 | Statistical histogram of the mine earthquake $0.5 \leq M_L < 1.0$ frequency.
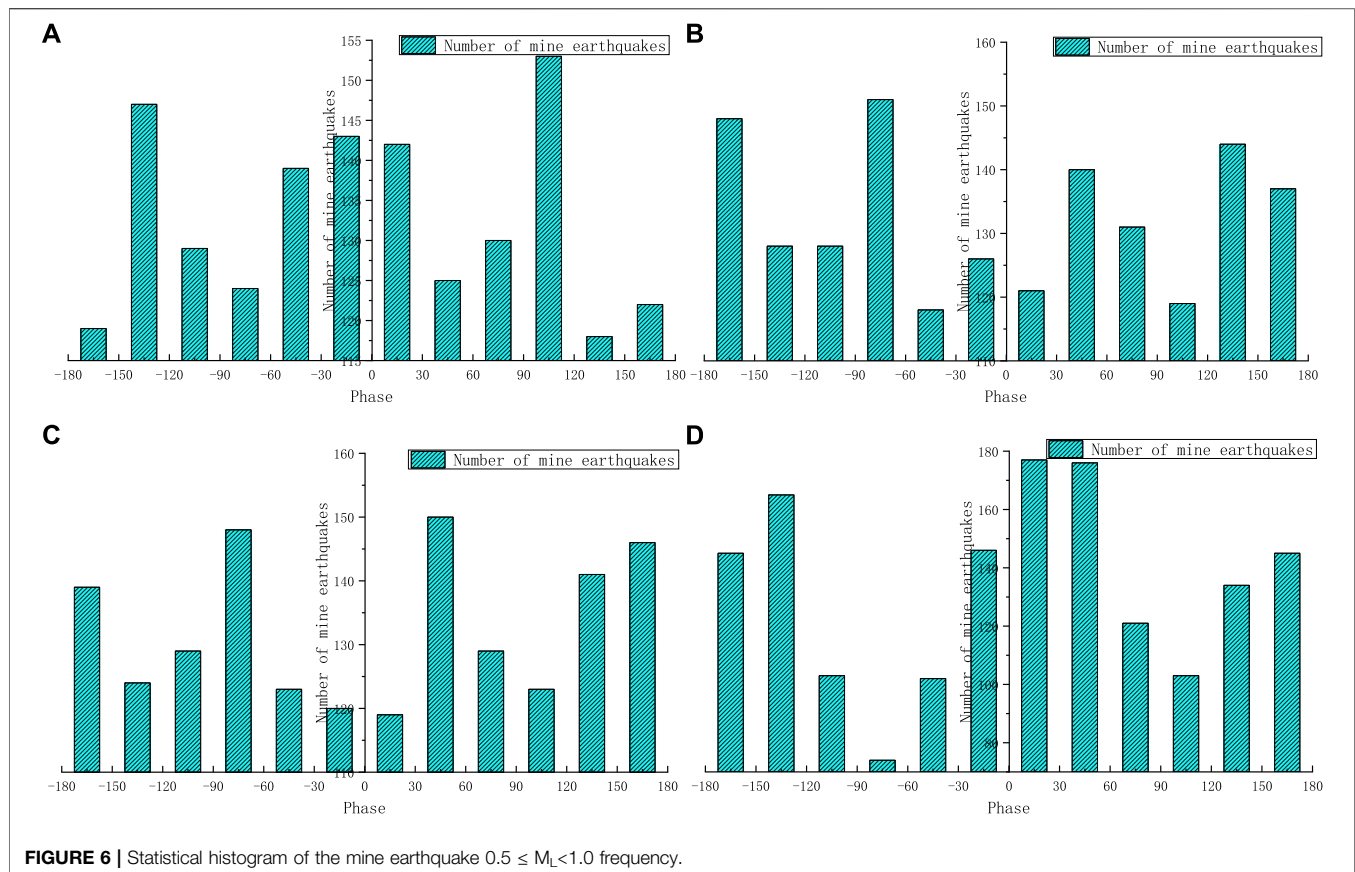
From the statistical results of the above-mentioned magnitude files, it is apparent there are differences in the triggering effects of solid tides on different levels of mine earthquakes. This level is the closest to the overall distribution trend in **Figure 4**, where the level of $M_L < 0$ is the discrete maximum, and the other levels are close to the general trend. Observing the p value result in **Figure 9** also shows this law. The statistical p value of the horizontal shear component of the mine earthquake is closer to 0.05, and the triggering effect is obvious. The vertical, east–west, and north–south components of mine earthquakes with $M_L < 0$ have p values close to 1. The corresponding statistical results of phase distribution are also very discrete, indicating that the occurrence of such a large-scale mine earthquake is not triggered by the earth's tide. Although the p value of other grades is greater than 0.05, the frequency distribution of the corresponding phase still maintains a more obvious regularity. In the corresponding statistical study of earthquakes, $p < 0.05$ is not the only criterion for the triggering of earth tides, and the distribution of earthquakes in the tidal phase is more important.

Although there are differences in the distribution of the phases of the various components of the earth's tides for mine earthquakes of different magnitudes, the overall law tends to be the same: relative to the vertical component, mine earthquakes mostly occur near the 0° and ±90° phases, and the distribution is closer to the 0° phase. For the east-west and north-south horizontal components, mine earthquakes occur more frequently near the phases of 0° and ±180° and are more widely distributed near the phases of ±180°. For the horizontal shear stress component, mine earthquakes occur frequently near the phases of 0° and ±180°, and with the change in magnitude, this stress component maintains a significant correlation with the triggering of mine earthquakes.

DISCUSSION OF THE TRIGGERING EFFECT OF TIDAL STRESS ON FLOOR-TYPE MINE EARTHQUAKES

Affected by the dynamic disturbance process of mining, the roof and floor of the coal seam have been undergoing dynamic evolution and adjustment. The development and evolution of the "three belts" in the roof; the periodic breakage of the roof and the appearance of periodic pressure; the bottom heave and protrusions in the floor; and impact, deformation, and destruction of the two gangs are all external manifestations of this dynamic evolution process. Regardless of whether it is the top floor or the two banks of surrounding rocks, the failure and instability processes are all based on the original stress state in the formation as the starting point. Under the effect of mining disturbance, the surrounding rock structure and its evolution process gradually approach or reach their "critical state" and then cause local damage or large-scale instability (Cui et al., 2022; Feng
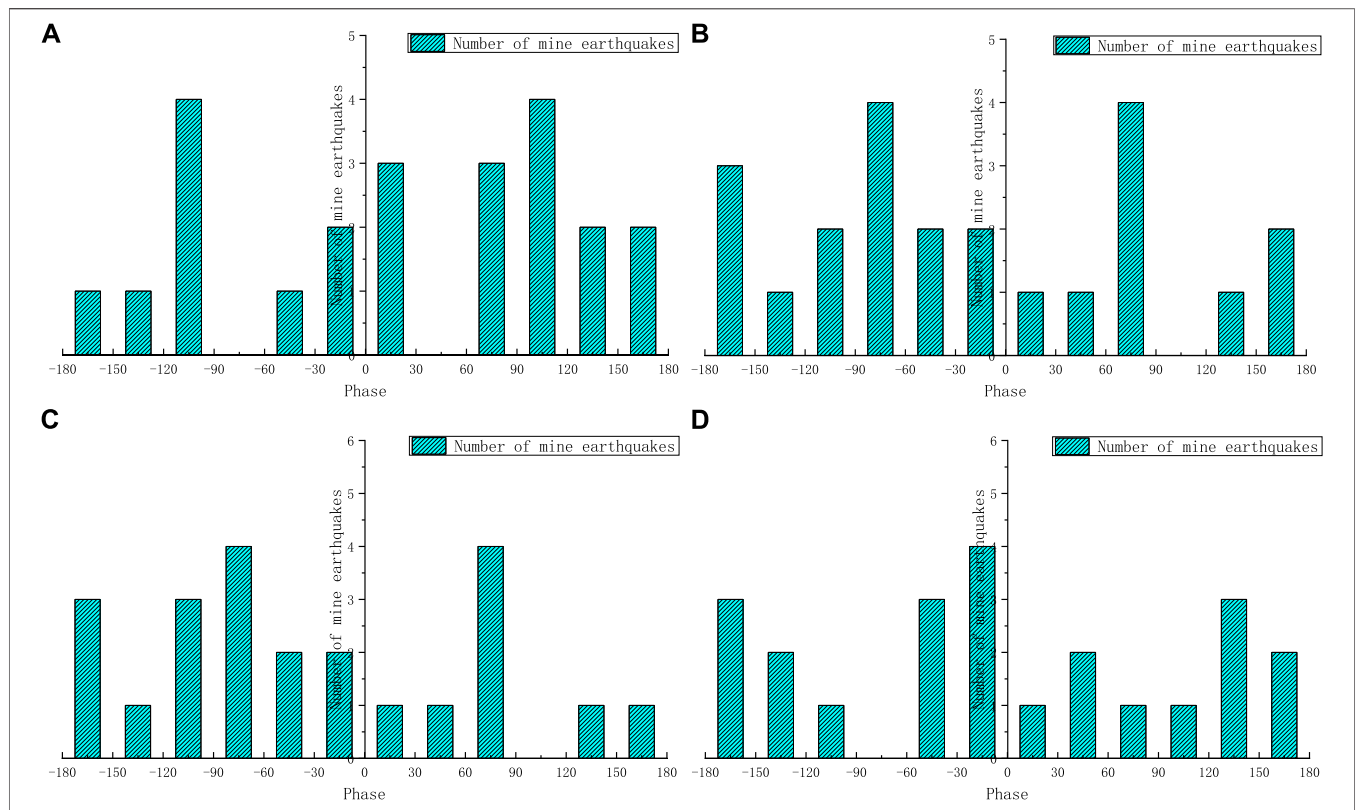
FIGURE 7 | Statistical histogram of the mine earthquake $1.0 \le M_L < 1.5$ frequency.
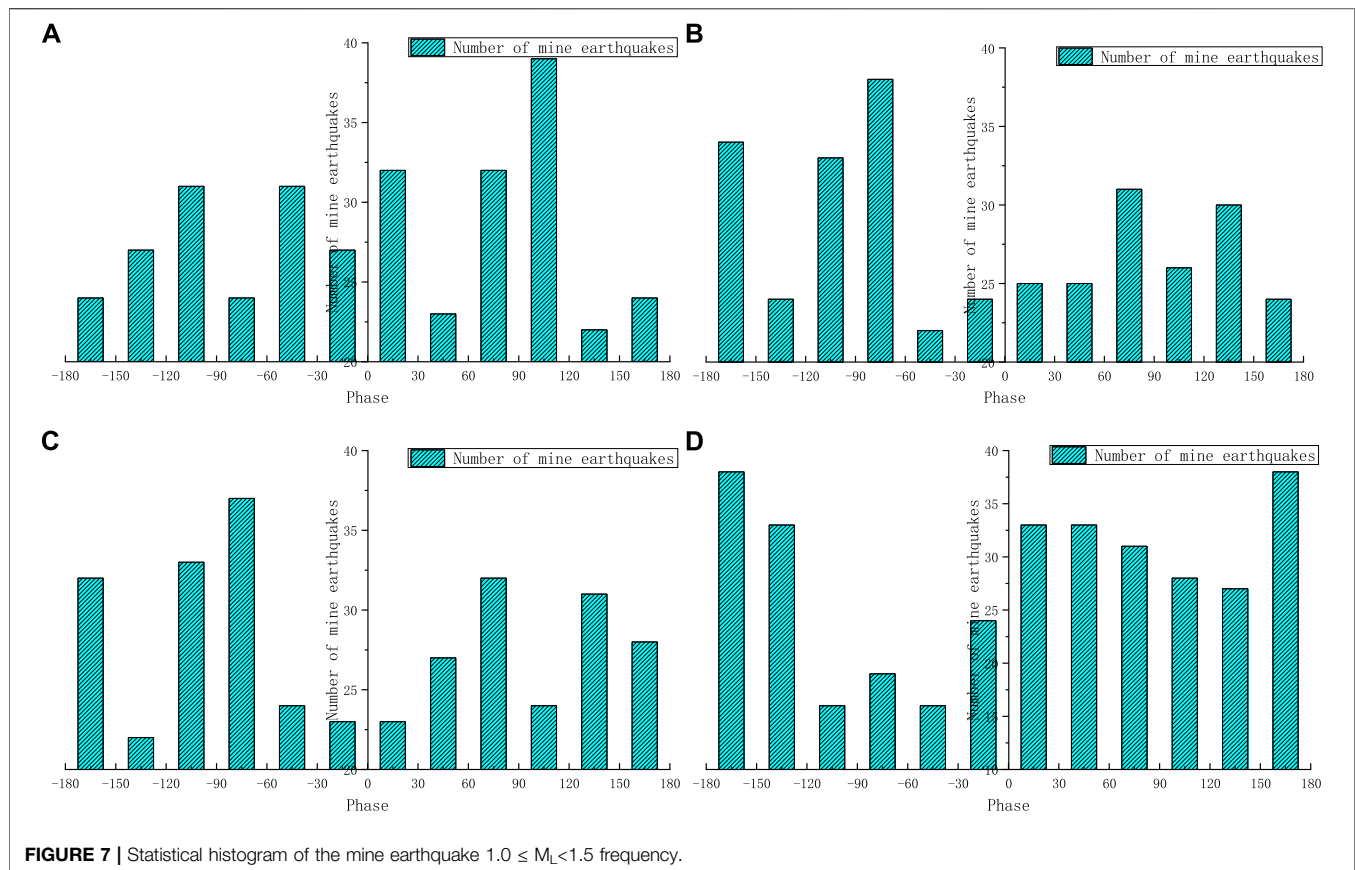
et al., 2022). Therefore, the emergence and evolution of "critical fracture zones" in roofs, floors, or roadways reflects the comprehensive action of multiple factors such as the overburden rock structure, original stress field, and mining disturbance. In particular, on the roof and floor, its incubation, expansion, and evolution processes intensively reflect multiple physical and mechanical fields and synergistic mechanisms and state evolution processes on multiple spatial scales.

In the mining process, affected by mining disturbance, the surrounding rock of the stope has been in a process of dynamic change. Among them, in the surrounding rock of the roof and floor, the stress state of certain areas will break due to reaching their critical conditions, which will cause a large number of microseismic events. The spatial distribution characteristics and dynamic evolution process of microseismic sources in the roof and floor also well reflect the temporal and spatial evolution process and law of the "critical fracture zone" in the surrounding rock of the roof and floor. In the mining process, the stress state and failure mode of the roof and floor of the coal seam are very different. Therefore, although the top plate and the top plate rupture, both show a common microseismic activity. However, the microseisms that occur on the top and bottom plates are very different in both the incubation environment, the induced mechanism, and the regional dynamic response. This difference also caused the obvious difference in the triggering

effect of the solid tidal stress on the roof and floor (Wu et al., 1999).

The spatial distribution characteristics and dynamic evolution process of microseismic sources in the roof and floor also better reflect the temporal and spatial evolution process and law of the "critical fracture zone" in the surrounding rock of the roof and floor. In the mining process, the stress state and failure mode of the roof and floor of the coal seam are very different. Therefore, although the top plate and the top plate rupture, both show a common microseismic activity. However, the microseisms that occur on the top and bottom plates are very different in both the incubation environment, the induced mechanism, and the regional dynamic response. This difference also caused the obvious difference in the triggering effect of the solid tidal stress on the roof and floor (Gao et al., 2021). According to the value of p in **Figure 9** and the literature (Zhang et al., 2016b), compared with roof-type mine earthquakes, the triggering effect of solid tide stress on floor-type mine earthquakes is smaller, which is also caused by the difference in the occurrence mechanism between the two.

Comparing the statistical results of the actual occurrence of mine earthquakes, it is found that the distribution characteristics of the phases of the tidal stress components of the mine earthquakes of different scales on the floor are consistent with the above-mentioned trigger mechanism. The occurrence of floor-type mine earthquakes is controlled by

FIGURE 8 | Statistical histogram of the mine earthquake $M_L > 1.5$ frequency.
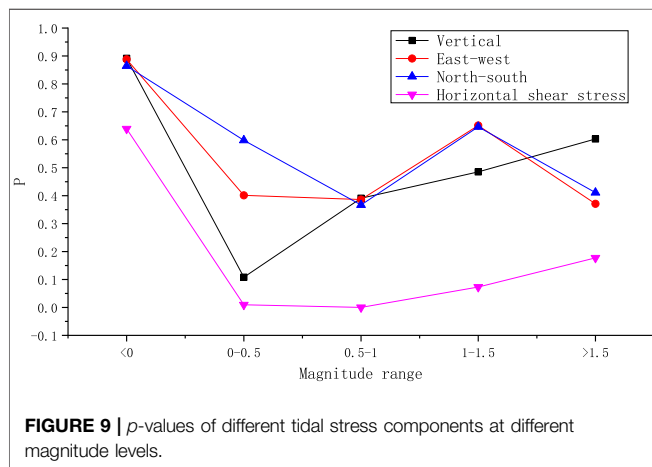
FIGURE 9 | *p*-values of different tidal stress components at different magnitude levels.

both the gravity field and the horizontal tectonic stress field. Taking the vertical component of tidal stress as a reference, mine earthquakes are most distributed near the 0° phase, and this type of mine earthquake is controlled by gravity; the frequency of mine earthquakes occurring near the ±180° phase is the second, and this type of mine earthquake is controlled by horizontal tectonic stress. This difference in quantity also shows that the gravity-controlled type of mine earthquakes that occurred on the coal seam floor of the Yanbei mining area accounted for the majority. At the same time, the cause of the

dual control of gravity and tectonic movement due to mining is also an important difference between it and the natural earthquake induced by the fault tectonic activity, so there are differences in response to the triggering action of solid tides (Xu et al., 2010; Yu et al., 2022).

The advance warning of a mine earthquake or rock burst has always been a difficult problem in coal mine safety mining. As an additional disturbance stress, solid tidal stress can only be triggered when the surrounding rock is in a critical state. Therefore, in engineering practice, the accuracy of prediction can be improved by combining monitoring technologies such as microearthquake, ground sound, and electromagnetic radiation. For example, when it is judged that the surrounding rock enters the critical state according to this monitoring information, the early warning parameters can be optimized according to the time-phase characteristics of solid tidal stress, which is also the focus of application research in the next step (Zhang et al., 2013).

CONCLUSION

1) As a "hidden" periodic change factor that occurs in the interior of the earth, solid tides have a significant triggering effect on the occurrence of floor-type mining earthquakes.

2) The triggering effects of tidal stress on different magnitudes of floor-type mine earthquakes are different, but the overall

trend is similar. In terms of phase distribution, most mine earthquakes occur near 0° and ±180° phases in vertical, east–west, north–south, and horizontal shear stress components of tidal stress.

3) The triggering mechanical effects of tidal stress on different types of mine earthquakes are different. There are mainly two types of gravity control: vertical type and horizontal stress control type in the floor. The former is prone to occur when the vertical component of tidal stress is the largest, and the latter is prone to occur when the east–west and north–south horizontal components are the largest. In the frequency of occurrence, the former is more common than the latter.

4) The statistical analysis of floor-type mine earthquakes shows that there is a correlation between the periodic micro-dynamic effects of solid tides in the crust and mine earthquake activities. This provides new ideas for revealing the incubation and triggering conditions of mine earthquakes. In the follow-up study, on the basis of the existing coal mine dynamic disaster early warning technology, the triggering effect of the earth's tide factor can be considered to improve the effectiveness of disaster early warning.

REFERENCES

Bucholc, M., and Steacy, S. (2016). Tidal Stress Triggering of Earthquakes in Southern California. *Geophys. J. Int.* 205 (2), 681–693. doi:10.1093/gji/ggw045

Chen, L., Chen, J. G., and Xu, Q. H. (2012). Correlations between Solid Tides and Worldwide Earthquakes <i>M</i><sub>S</sub> ≥ 7.0 since 1900. *Nat. Hazards Earth Syst. Sci.* 12 (3), 587–590. doi:10.5194/nhess-12-587-2012

Chen, X. H., Li, W. Q., and Song, W. H. (2006). Analysis of Celestial Body's Activity on Crustal Stress and Rock Burst. *J. Liaoning Tech. Univ.* 25 (05), 652–654. doi:10.3969/j.issn.1008-0562.2006.05.004

Cui, G. D., Wang, W. X., Dou, B., and Li, Y. (2022). Geothermal Energy Exploitation and Power Generation via a Single Vertical Well Combined with Hydraulic Fracturing. *J. Energy Eng.* 148 (1). doi:10.1061/(ASCE)EY.1943-7897.0000809

Feng, G. L., Chen, B. R., Xiao, Y. X., Jiang, Q., Li, P-X., Zheng, H., et al. (2022). Microseismic Characteristics of Rockburst Development in Deep TBM Tunnels with Alternating Soft–Hard Strata and Application to Rockburst Warning: A Case Study of the Neelum–Jhelum Hydropower Project. *Tunn. Undergr. Space Technol.* 122, AR 104398. doi:10.1016/j.tust.2022.104398

Feng, G.-L., Feng, X.-T., Chen, B.-r., Xiao, Y.-X., and Yu, Y. (2015). A Microseismic Method for Dynamic Warning of Rockburst Development Processes in Tunnels. *Rock Mech. Rock Eng.* 48 (5), 2061–2076. doi:10.1007/s00603-014-0689-3

Gao, M. Z., Xie, J., Gao, Y. N., Wang, W., Li, C., Yang, B., et al. (2021). Mechanical Behavior of Coal under Different Mining Rates: A Case Study from Laboratory Experiments to Field Testing. *Int. J. Min. Sci. Technol.* 31 (5), 825–841. doi:10.1016/j.ijmst.2021.06.007

Glasby, G. P., and Kasahara, J. (2001). Influence of Tidal Effects on the Periodicity of Earthquake Activity in Diverse Geological Settings with Particular Emphasis on Submarine Hydrothermal Systems. *Earth-Science Rev.* 52 (04), 261–297. doi:10.1016/s0012-8252(00)00031-3

Guo, G. C., and Yang, Y. K. (2021). Study on the Mechanism of Rockburst Induced by Tidal Force. *J. Taiyuan Univ. Technol.* 52 (04), 534–541. doi:10.16355/j.cnki.issn1007-9432tyut.2021.04.004

Kano, Y., and Yanagidani, T. (2006). Broadband Hydroseismograms Observed by Closed Borehole Wells in the Kamioka Mine, Central Japan: Response of Pore Pressure to Seismic Waves from 0.05 to 2 Hz. *J. Geophys. research-solid earth* 111 (B3). doi:10.1029/2005jb003656

Li, J., Jiang, H. K., Huang, Y., Qu, J-h., and Gao, C-j. (2014). Statistical Analysis on Tidal Triggering of Recent Earthquakes in the Tianshan Seismic Zone. *Earthquake* 34 (02), 35–44. doi:10.3969/j.issn.1000-3274.2014.02.004

Li, T., Cai, M. F., and Cai, M. (2006). A Discussion on Classification of Mining-Induced Seismicity. *Chin. J. Rock Mech. Eng.* 25 (s2), 3679–3686. doi:10.3321/j.issn:1000-6915.2006.z2.054

Li, T., Zhang, J. W., Lv, Y. G., Zhou, P., Qiao, Z-D., and Chen, S. H. (2011). Relationship between Mining and Mining-Induced Seismicity. *J. China Coal Soc.* 36 (12), 2127–2132. doi:10.13225/j.cnki.jccs.2011.12.031

Luo, Y., Tao, W. B., Ma, H. F., Tao, J., and Hou, J. L. (2015). Mechanism of the Astro-Tidal-Triggering to Coal and Gas Outburst. *Chin. J. Rock Mech. Eng.* 34 (s1), 3005–3011. doi:10.13722/j.cnki.jrme.2014.0826

Metivier, L., De Viron, O., Conrad, C. P., Renault, S., Diament, M., and Patau, G. (2009). Evidence of Earthquake Triggering by the Solid Earth Tides. *Earth Planet. Sci. Lett.* 278 (3-4), 370–375. doi:10.1016/j.epsl.2008.12.024

Pan, J. F., Qi, Q. X., Liu, S. H., Wang, S. W., Ma, W. T., and Kang, X. C. (2020). Characteristics, Types and Prevention and Control Technology of Rock Burst in Deep Coal Mining in China. *J. China Coal Soc.* 45 (1), 111–121. doi:10.13722/j.cnki.jrme.2014.0826

Sun, C. Q., Yan, C. H., Wu, X. P., and Xu, Y-j. (2014). The Effect of Tidal Triggering on Seismic Fault in Eastern Tibetan Plateau and its Neighboring Areas. *Chin. J. Geophys.* 57 (02), 2054–2064. doi:10.6038/cjg20140703

Wu, K., Ji, C., Luo, L., and Wang, X. (2020). Simulation Study of Moon-Based InSAR Observation for Solid Earth Tides. *Remote Sens.* 12 (1). doi:10.3390/rs12010123

Wu, X. P., Mao, W., Huang, Y., and Jiang, J. (1999). Statistical Analysis of Tidal Stress Effect on Seismic Faults. *Chin. J. Geophys.* 42 (s1), 65–74.

Xie, H. P., Gao, F., and Ju, Y. (2015). Research Review of the State Key Research Development Program of China: Deep Rock Mechanics and Mining Theory. *Chin. J. Rock Mech. Eng.* 34 (11), 2161–2178. doi:10.13722/j.cnki.jrme.2015.1369

Xiong, Z. Y., Xie, Z. Z., Lei, X. L., Fu, H., and Ma, Q. B. (2015). Triggering Relationship between Seismic Activity and Tidal Stress in Dayao-Yaoan and its Adjacent Area of Yunnan Province. *J. Seismol. Res.* 38 (01), 66–74. doi:10.3969/j.issn.1000-0666.2015.01.009

Xu, X. F., Dou, L. M., Liu, J., Cui, X-h., Zhang, Y-l., and Yao, X-y. (2010). Research of Reasons and Controlling for Floor Burst in Coal Mine Roadway. *Rock Soil Mech.* 31 (6), 1977–1982. doi:10.16285/j.rsm.2010.06.001

Yu, Y., Zhao, D. C., Feng, G. L., Geng, D-X., and Guo, H-S. (2022). Energy Evolution and Acoustic Emission Characteristics of Uniaxial Compression

DATA AVAILABILITY STATEMENT

The original contributions presented in the study are included in the article/supplementary material; further inquiries can be directed to the corresponding author.

AUTHOR CONTRIBUTIONS

YZ and HJ conceived and designed the methods, provided the guide of theoretical research for the study, completed the data analysis, and economically supported the project. HW completed the data collection.

FUNDING

Failure of Anchored Layered Sandstone. *Front. Earth Sci.* 10, AR 841598. doi:10.3389/feart.2022.841598

Yuan, L. (2021). Research Progress of Mining Response and Disaster Prevention and Control in Deep Coal Mines. *J. China Coal Soc.* 46 (3), 716–725. doi:10.13225/j.cnki.jccs.YT21.0158

Zahran, K. H., Jentzsch, G., and Seeber, G. (2005). World-wide Synthetic Tide Parameters for Gravity and Vertical and Horizontal Displacements. *J. Geodesy* 79 (6-7), 293–299. doi:10.1007/s00190-005-0460-3

Zhang, R., Jiang, Z. Q., Li, X. H., Chao, H. D., and Sun, J. (2013). Study on the Failure Depth of Thick Seam Floor in Deep Mining. *J. China Coal Soc.* 38 (01), 67–62. doi:10.13225/j.cnki.jccs.2013.01.024

Zhang, Y. Z., Ji, H. G., Cai, M. F., Li, T., and Xiang, P. (2016b). Triggered Effect of Solid Tidal Stress on Rockburst and its Mechanism. *J. Min. Saf. Eng.* 33 (03), 535–543. doi:10.13545/j.cnki.jmse.2016.03.024

Zhang, Y. Z., Ji, H. G., Peng, H., and Xiang, P. (2016a). Correlation between Rockburst and Regional Tectonic Stress Environment and its Strain Response Characteristics. *J. China Coal Soc.* 41 (S2), 311–318. doi:10.13225/j.cnki.jccs.2015.1473

Zhou, J. C., Sun, H. P., Xu, J. Q., and Chen, X-D. (2013). Tidal Strain and Tidal Stress in the Earth's Interor. *Chin. J. Geophys.* 56 (11), 3779–3787. doi:10.6038/cjg20131119

Zhu, C., He, M. C., Zhang, X. H., Tao, Z. G., Yin, Q., and Li, L. F. (2021). Nonlinear Mechanical Model of Constant Resistance and Large Deformation Bolt and Influence Parameters Analysis of Constant Resistance Behavior. *Rock Soil Mech.* 42 (07), 1911–1924. doi:10.16285/j.rsm.2020.1764